Preparation and Characterization of Lignin-TiO_2 UV-shielding Composite Material by Induced Synthesis with Nanofibrillated Cellulose

Daliang Guo,[a,c,*] Jinmeng Zhang,[b] Lizheng Sha,[a] Bei Liu,[a,*] Xin Zhang,[a] Xiumei Zhang,[b] and Guoxin Xue [b]

It is desirable to develop biodegradable ultraviolet (UV)-shielding materials from renewable resources, as the demand for sustainability is ever increasing. In this work, a novel lignin-TiO_2 UV-shielding composite was synthesized successfully *via* a hydrothermal method induced by nanofibrillated cellulose (NFC). Comprehensive characterization showed that the lignin-TiO_2@NFC composite induced by NFC had good nanoparticle size, shape, and thermal stability. The sunscreen performance of lignin-TiO_2@NFC was investigated *via* mixture with unmodified hand cream. The UV-visible (vis) transmission spectra results revealed that the unmodified cream with 10 wt% lignin-TiO_2@NFC absorbed approximately 90% of UV light in the full UV band (200 nm to 400 nm), which indicated that lignin-TiO_2@NFC had a good UV-shielding ability.

Keywords: TiO_2; Lignin; Cellulose nanofibril; UV-shielding

Contact information: a: School of Environmental and Natural Resources, Zhejiang University of Science and Technology, Hangzhou, China; b: College of Textile Science and Engineering, Zhejiang Sci-Tech University, Hangzhou, China; c: Key Laboratory of Pulp and Paper Science and Technology of the Ministry of Education of China, Qilu University of Technology, Jinan, China;
** Corresponding authors: 08guodaliang@163.com; 08liuxiaobei@163.com*

INTRODUCTION

In recent years, the amount of ultraviolet (UV) radiation has increased with the destruction of the ozone layer, and the overexposure of UV radiation causes negative effects on human health and material stability (Slaper *et al*. 1996; Dong *et al*. 2018). Therefore, the research and development of UV-shielding materials has aroused extensive interest in academia and industry. In this field, titanium dioxide (TiO_2) is widely investigated as an inorganic UV-shielding agent due to its ability to reflect, scatter, and absorb a wide range of ultraviolet radiation (Sambandan and Ratner 2011). However, the poor dispersibility and strong photocatalytic degradation hazard of TiO_2 impair its application (Xiao *et al*. 2013).

In the process of preparing TiO_2 by traditional sol-gel method, nucleation and the growth of secondary particles in the precipitation process cannot be well controlled. In addition, nanoparticles agglomerate easily, and this method requires sintering to obtain crystals, so their structure cannot be easily controlled (Dinh *et al*. 2009). The generation of TiO_2 with suitable particle size and good dispersibility *via* a simple and fast method is a research area of great interest (Rockafellow *et al*. 2009; Zhou and Fu 2013). The template method can effectively control the morphology, structure, and size of synthesized nanomaterials, so it has become an important method of preparing nanomaterials (Giese *et*

al. 2015). Dong *et al*. (2002) used the polymer template with a groove structure and found that TiO_2 sol infiltrated with appropriate concentration can be used to obtain fibrous TiO_2 after solvent evaporation, but the polymer material is difficult to obtain with this method.

As it is a natural high polymer, nanocellulose is also used as a template for the preparation of nano-TiO_2. Several studies have reported the successful application of cellulose templates in the preparation of TiO_2 with specific morphology. The two main features of cellulose templates are a uniform network formed in aqueous solution and nucleation sites formed by a large amount of surface hydroxyl groups (Marques *et al*. 2006). Miao *et al*. (2006) dispersed cellulose in titanium tetrabutyloxide to prepare TiO_2 of 10 nm to 20 nm size. In addition, Zhou *et al*. (2007) used cellulose nanocrystals (CNC) as a morphology inducer to synthesize square nano-TiO_2. Wei *et al*. (2012) used CNC to prepare mesoporous TiO_2 in different shapes. The authors claimed that reactions between the hydroxyl groups of the long-chain CNC and TiO_2 precursor provided a physical barrier to prevent the growth and aggregation of the TiO_2 precursor and promote the spherical structure by self-assembly. Chen *et al*. (2016a) prepared TiO_2 composite material with high dispersion, small grain size, and high specific surface area induced by CNC.

Studies have demonstrated that inorganic TiO_2 nanoparticles have some side effects in sunscreen materials (Zaccariello *et al*. 2017). In sunlight, inorganic TiO_2 nanoparticles have photocatalytic activity that produces reactive species, such as O_2- and OH radicals and other reactive oxygen species (ROS), such as H_2O_2, which can damage cellular components, including DNA, proteins, lipids, and membranes (Sander *et al*. 2002). To eliminate the photocatalytic activity of TiO_2, inorganic or polymeric thin layers have been coated onto the surface of TiO_2 nanoparticles. The inorganic coating layers included zeolite, silica, and alumina (Jaroenworaluck *et al*. 2006; Shen *et al*. 2006; Zhang *et al*. 2009).

Excessive use of inorganic coatings could lead to poor light transmittance in the UV-screening product. Inorganic particles are not easily dispersed in creams, which greatly limits their application in skincare products. Morlando *et al*. (2018) utilized the antioxidant properties of chitosan to capture the free radicals generated by the photocatalytic activity of TiO_2. However, the prepared chitosan/TiO_2 nanocomposite particles had weak UV absorption capacity.

Lignin is the most abundant aromatic polymer (Kai *et al*. 2016). It has a natural phenylpropane skeleton and contains functional groups such as phenolic hydroxyls, double bonds, and carbonyls. The structural properties of lignin suggest that it has excellent free radical scavenging ability, good UV-absorption, and antioxidant properties (Pan *et al*. 2006; Qian *et al*. 2016; Li *et al*. 2018). Hambardzumyan *et al*. (2012) used lignin as a UV-shielding material, and they reported the use of a UV-blocking nanocomposite coating based on lignin that exhibited high transmittance in the visible spectrum. The use of lignin to capsulate chemical sunscreens improves the UV-blocking performance of chemical sunscreens. In addition, lignin has been employed to modify the properties of TiO_2. Nair *et al*. (2016) combined lignin with TiO_2 *via* a ball-milling method. The composite obtained by this method had low thermal stability and poor UV-shielding. Chen *et al*. (2016b) prepared lignin/TiO_2 UV-shielding composite material *via* a sol gel method, and they found that the precursor of TiO_2 was bound with the oxygen-containing functional groups in lignin and formed stable complexes during the hydrolysis process. Morsella *et al*. (2016) prepared lignin/TiO_2 composites *via* UV irradiation in THF (tetrahydrofuran) solution, and they found that lignin can effectively reduce the photocatalytic activity of TiO_2. However, large amounts of organic solvents, such as tetrahydrofuran and glutaraldehyde, were used,

but these are toxic and not suitable for skincare products (Li *et al*. 2019). The study of UV-shielding of lignin showed that lignin exhibited antioxidant properties and acted as a free radical scavenger due to the presence of the phenolic hydroxyl groups; the phenolic hydroxyl groups also act as a proton donor and can stabilize the resulting radicals *via* substituents and delocalization (Sun *et al*. 2014). Ibrahim *et al*. (2019) employed lignin to scavenge the hydroxyl radicals generated from the photocatalytic activity of TiO_2 by forming a lignin/TiO_2 composite. The results showed that lignin can reduce phototoxicity and scavenge the hydroxyl radicals. Therefore, the use of lignin replacing the inorganic coating to modify TiO_2 improves the UV-blocking performance of chemical sunscreens and may enhance the antioxidant properties of chemical sunscreens. It is a great idea to use NFC, taking advantage of its characteristic functional groups and orderly spatial structure, together with lignin, to induce TiO_2 crystal growth and control the particle size, while completing the surface lignin coating at the same time.

In this study, multi-hydrogen-bond reticulated NFC was prepared with high dispersion through enzymatic hydrolysis and high-pressure homogenization. Lingin-TiO_2 composite materials were prepared by using NFC as the inducer and an alkali lignin one-step solvothermal method. The influences of UV-shielding properties, antioxidant properties, thermal stability, and the dynamic mechanical properties of the composite material were studied. The composite materials can be added to skin care products and has excellent anti-ultraviolet ability and good application prospect.

EXPERIMENTAL

Materials

The NFC suspension (solid content was 1.08%) used bleached softwood pulp as the raw material, and it was made with 68.9 MPa (10,000 psi) and homogenized 10 times by using the microjet high pressure homogeneous machine (LMZO; Microfluidics International Corporation, Newton, MA, USA). The diameter of the resulting NFC was about 87 nm. The alkali lignin (solubility: H_2O, pH: 10.5) was purchased from Sigma-Aldrich (Shanghai, China). The titanium butoxide, which was 98% pure, was obtained from Mike Chemical Instrument Co. Ltd. (Hangzhou, China). The unmodified hand cream used was Dabao SOD hand cream, which was purchased from Dabao Cosmetics Co. LTD (Beijing, China); its main ingredients contain glycerin and silicone oil.

Synthesis of TiO_2 and TiO_2@NFC

The TiO_2 precursor was prepared *via* the solvothermal method. Five mL of titanium butoxide (5.0 g) was introduced into 25 mL of anhydrous ethanol, and the mixed solution was stirred with a magnetic stirrer at room temperature at 400 r/min for 30 min. Then, 10 mL of the NFC suspension (solid content was 1.08%) was slowly added, and stirring continued until white clouding occurred. Next, the suspension liquid was transferred to the high temperature and high-pressure reactor for reaction at 120 ° for 2 h. Colloids were allowed to form for 24 h at room temperature. Finally, the gel was dried under a vacuum for 12 h. The powder obtained from grinding in the mortar was nano-TiO_2 induced by nanocellulose and used without further purification; it was named TiO_2@NFC. For comparison, TiO_2 samples were prepared according to the above preparation method by replacing the nanocellulose suspension with 10 mL of H_2O.

Synthesis of Lignin-TiO_2@NFC

Five mL of titanium butoxide (5.0 g) was introduced into 25 mL of anhydrous ethanol, and the mixed solution was stirred with a magnetic stirrer at room temperature at 400 r/min for 30 min. Then, 0.1 g of alkali lignin was added to the 10 mL of NFC suspension with stirring. Next, all suspension liquid was transferred to the high temperature and high-pressure reactor for reaction at 120 °C for 2 h. The colloids were allowed to form for 24 h at room temperature. Finally, the gel was dried under a vacuum for 12 h. Finally, the resultant yellow powder was the lignin-TiO_2 composite; it was named lignin-TiO_2@NFC.

X-ray Diffraction (XRD) Analysis

The crystal structure of TiO_2 and the composite material hybrids were recorded with an X-ray diffractometer (XRD, Bruker D2 Phaser, Bruker Corp., Karlsruhe, Germany). The scanning angle (2θ) ranged from 10° to 80° with a step increment of 0.02°.

Fourier Transform Infrared (FT-IR) Spectroscopy Analysis

The FT-IR spectra of the TiO_2 and the prepared composite material hybrids were obtained on a Fourier transform infrared spectrometer (NICOLET5700; Thermo Fisher Scientific, Madison, WI, USA) using a KBr disc containing finely ground samples (1 %). Ten scans were taken for each sample recorded from 4000 cm^{-1} to 400 cm^{-1} with a resolution of 0.5 cm^{-1}.

Scanning Electron Microscopy (SEM) Analysis

The morphology analysis of the TiO_2@NFC and lignin-TiO_2@NFC were recorded with a scanning electron microscope (JSM-5610LV; JEOL Ltd., Tokyo, Japan).

X-ray photoelectron spectroscopy (XPS)

X-ray photoelectron spectroscopy (K-Alpha; Thermo Fisher Scientific, Madison, WI, USA) equipped with a monochromatic Al Kα X-ray source (1486.6 eV) was utilized to characterize the elemental chemical states of lignin-TiO_2@NFC.

Thermogravimetric Analysis (TGA)

The thermal analysis (TGA) and differential thermal analysis (DTG) of the TiO_2@NFC and lignin-TiO_2@NFC were conducted on a thermal analyzer (PYRIS I; PerkinElmer, Waltham, MA, USA). Four mg of lignin was placed on an aluminum crucible and heated from 25 °C up to 800 °C at a heating rate of 10 °C/min under a nitrogen atmosphere (40 mL/min).

UV-blocking Performance

The solid particles (TiO_2@NFC and lignin-TiO_2@NFC) were added to the hand cream in different mass ratios and stirred for 8 h to make a uniform sunscreen. A 3M (Hangzhou, China) medical porous tape with an area of 12.5 cm^2 was pasted on a clean transparent quartz plate with a thickness of 2 mm, and the sunscreen sample was evenly coated on the tape. The tape sample was placed in a dark place and dried for 30 min. The ultraviolet transmittance of samples at 290 nm to 400 nm was measured with a UV-visible (UV-vis) spectrometer (Cary 60; Agilent Technologies Co., Ltd., Palo Alto, USA).

RESULTS AND DISCUSSION

X-ray Diffraction

The XRD patterns of the composite material hybrids are shown in Fig. 1. The diffraction angles of 25.4°, 37.9°, 47.9°, 53.9°, 55.1°, 62.7°, 68.8°, 69.9°, and 75.5° corresponded to the (101), (004), (200), (105), (211), (204), (116), (220), and (215) interplanes of the anatase TiO_2 phase (JCPDS No. 21- 1272). Figure 1 shows the XRD patterns of the cellulose nanofibers with the TiO_2 coating and the lignin coating. As demonstrated in the XRD patterns, some XRD peaks of the composite materials were still identifiable by referring to JCPDS No. 21- 1272 due to the low crystallinity of the NFC (Zhang *et al*. 2019). Since lignin is amorphous in nature and lacks ordered structure, the XRD diffractograms of both composites did not show any diffraction peak and that can be referred to lignin, and no other crystalline by-products are formed even after the formation of lignin-TiO2@NFC composite (Ibrahim *et al*. 2019). The results showed that the TiO_2@NFC and lignin-TiO_2@NFC had increased crystalline structures, which may have been due to the fact that NFC is more malleable and spatial than TiO_2 because of its silk-like and broom-like structure; in addition, the hydrogen bonds in NFC are stronger, and chemical bonds are more frequent, which results in a better induction effect (Chu *et al*. 2019).

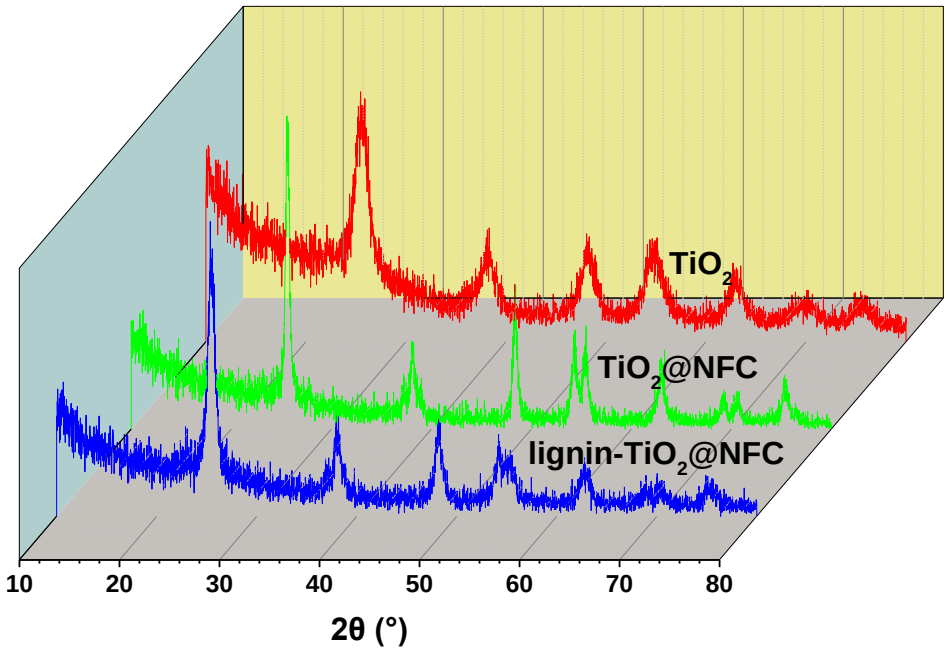

Fig. 1. The XRD patterns of the prepared composite materials

Many hydroxyl groups on the surface of NFC can form hydrogen bonds with $TiOH^{3+}$ and adsorb on the surface of the TiO_2 crystal unit, which promotes heterogeneous nucleation and growth of crystals. Therefore, structured TiO_2 nanocrystalline can be induced under relatively low temperature and simple conditions. The specific mechanism is shown in Fig. 2.

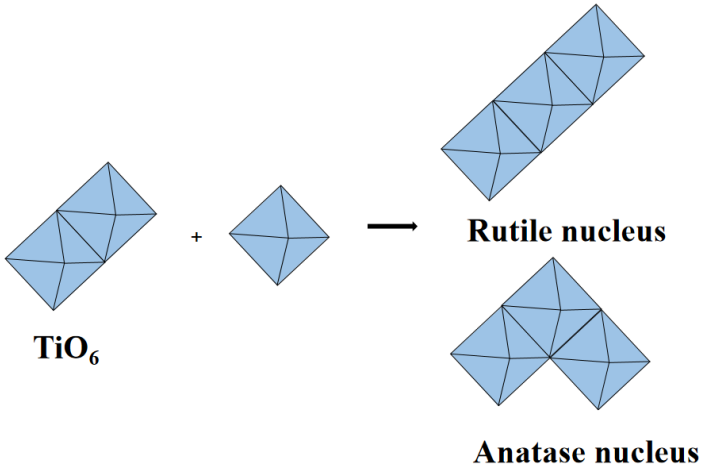

Fig. 2. The schematic illustration of the evolution process of the TiO_2 crystal

The steric resistance effect caused by the adsorption of NFC on the surface of the TiO_2 crystal unit affects the stacking mode of the third TiO_6 octahedron, and the third Tio_6 octahedron is more inclined to connect with the second TiO_6 octahedron from the back. Therefore, this promoted the generation of an anatase phase with a folded linear structure, and NFC and CNC were nano-sized in both the length and width directions. In addition, NFC was uniformly prepared under high pressure, with better solubility, a larger specific surface area, more exposed hydroxyl groups, and a free anion terminal, which created electrostatic interaction with Ti^{4+}. Therefore, the crystals prepared under double steric hindrance were better.

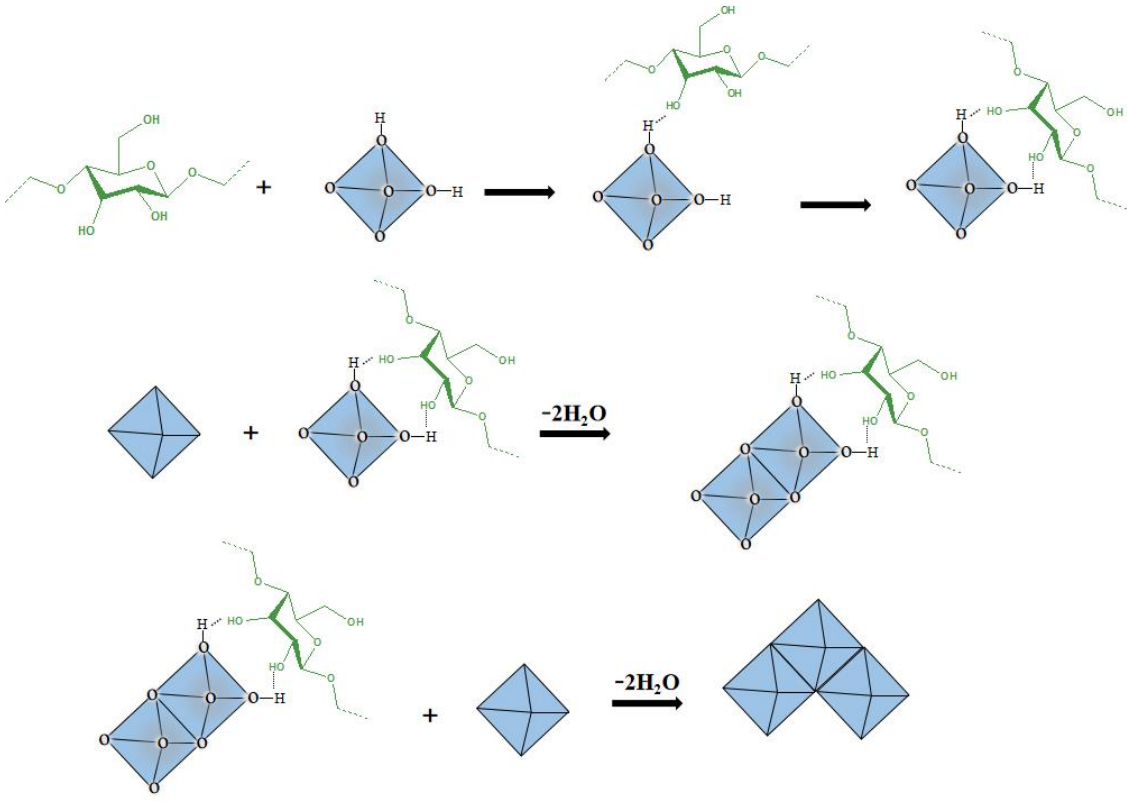

Fig. 3. The proposed mechanism of the evolution process of TiO_2 crystals in the presence of NFC

FT-IR Analysis

Figure 4 presents the FT-IR spectra of the pure TiO_2 and the prepared composite material hybrids. Broad and strong bands at 3430 cm^{-1} were observed for all samples, and they were attributed to the hydroxyl groups in the phenolic and aliphatic structures of lignin. Compared with that of lignin, the spectrum of lignin-TiO_2@NFC exhibited a new board absorption band in the range 400 cm^{-1} to 800 cm^{-1}, which was due to the stretching vibration of the Ti-O bands (Li *et al*. 2011). In addition, one single band at approximately 1631 cm^{-1} was also found for lignin-TiO_2@NFC hybrid due to the bending vibration of Ti-O bands. This indicated the formation of intermolecular hydrogen bonding between groups of the lignin surface and the TiO_2 surface (Hu *et al*. 2007). Combined with the above results, the composite materials were prepared successfully *via* cellulose nanofibril induction.

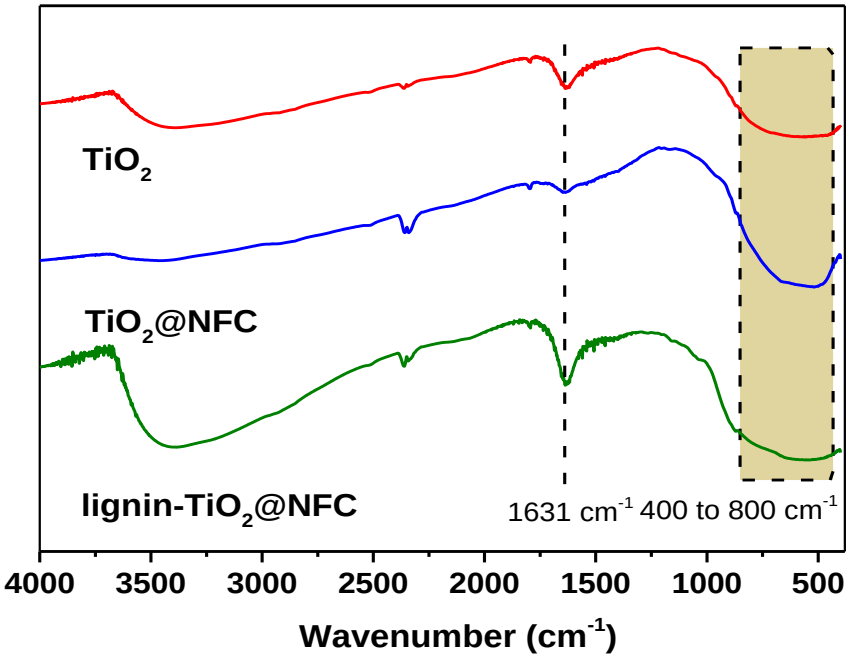

Fig. 4. The FT-IR spectra of TiO_2 and the prepared composite materials

SEM Analysis

Figure 5 shows that the TiO_2@NFC prepared by the NFC-induced synthesis had a uniform nanometer size, and the lignin-TiO_2@NFC composite material prepared with the same method increased in size. The size and degree of agglomeration of the composite materials were better than those reported by Morsella *et al*. (2016). As demonstrated in Fig. 5, the introduction of NFC solved the aggregation problem of TiO_2 and induced the formation of lignin-TiO_2@NFC composite material in a flake shape due to its special structure and chemical properties. Compared to nanoparticles with a spherical structure, the lamellar structure of lignin-TiO_2@NFC has a UV shielding effect, and a better UV shielding effect can be achieved with lignin-TiO_2@NFC with a small amount of doping (Chen *et al*. 2019). Because it does not affect the physical stirring of the blank cream, it can alleviate the danger of nanoparticle infiltration, such as penetrating into facial skin and greatly improve safety.

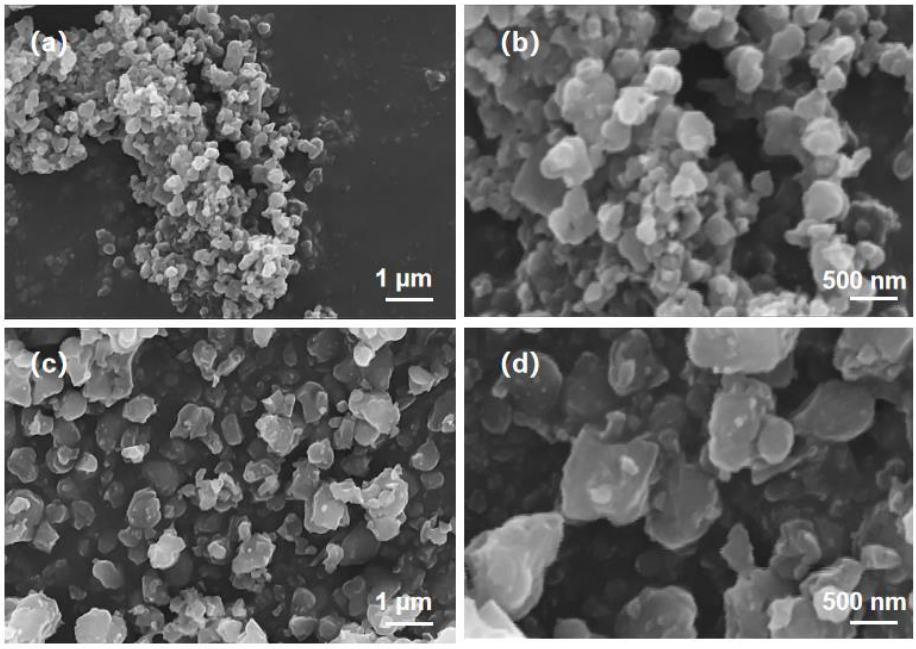

Fig. 5. The SEM images of the composites: (a) TiO_2@NFC × 20.0k; (b) TiO_2@NFC × 50.0k; (c) lignin-TiO_2@NFC × 20.0k; (d) lignin-TiO_2@NFC × 50.0k

The preparation mechanism of the small grain size and high activity titanium dioxide with cellulose nanofibril as the template is shown in Fig. 6.

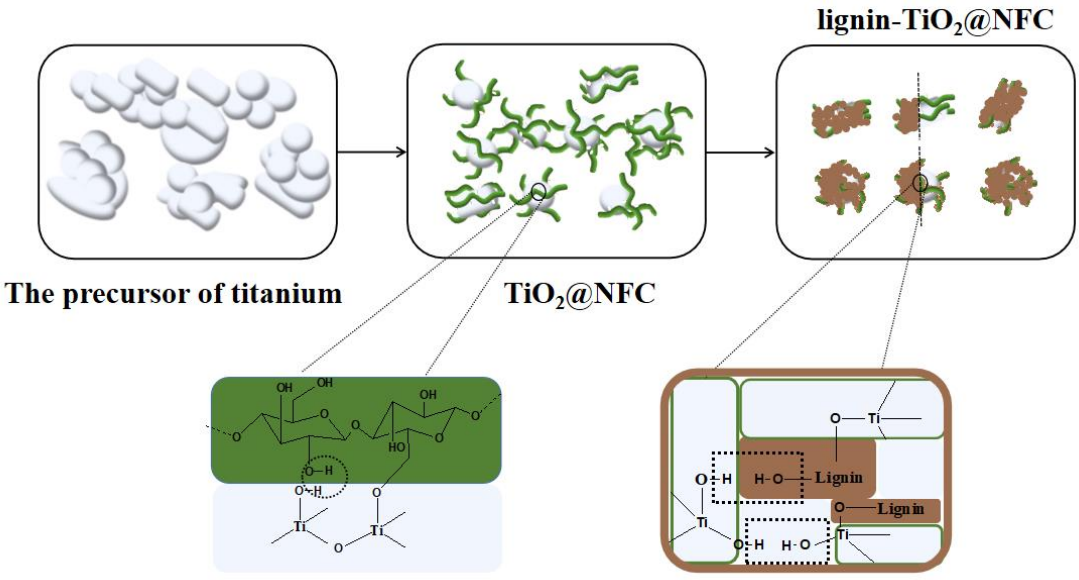

Fig. 6. Preparation mechanism of the novel Lignin-TiO_2 induced with NFC

Because they were affected by the hydroxyl groups of NFC macromolecules, the growth and aggregation of TiO_2 precursor were inhibited. Lignin also plays a role in promoting and inducing the crystallization of titanium dioxide due to its phenolic hydroxyl group and spatial structure. The composite materials achieved uniform immobilization and coating structure of titanium dioxide induced by lignin and cellulose. Nanoscale composite

materials were obtained without subsequent treatment to weaken the photocatalytic effect of lignin in the subsequent composite materials on titanium dioxide and the synergistic anti-ultraviolet effect.

XPS Analysis

The chemical composition of the lignin-TiO_2@NFC was elucidated by XPS. The XPS survey spectra of the lignin-TiO_2@NFC confirm that the lignin-TiO_2@NFC contains the elements of C, O, and Ti, as shown in Fig. 7a. In Fig. 7b, the main peak locked at 284.3 eV is assigned to C-C bonds, whereas the other peak at 285.6 eV corresponds to C-O bonds. The presence of carbon-oxygen polar bonds can contribute to the absorption of the Ti precursor and the nucleation of the TiO_2 nanoparticles on the surface of NFC (An *et al.* 2007). The O1s spectra of lignin-TiO_2@NFC is shown in Fig. 7c.

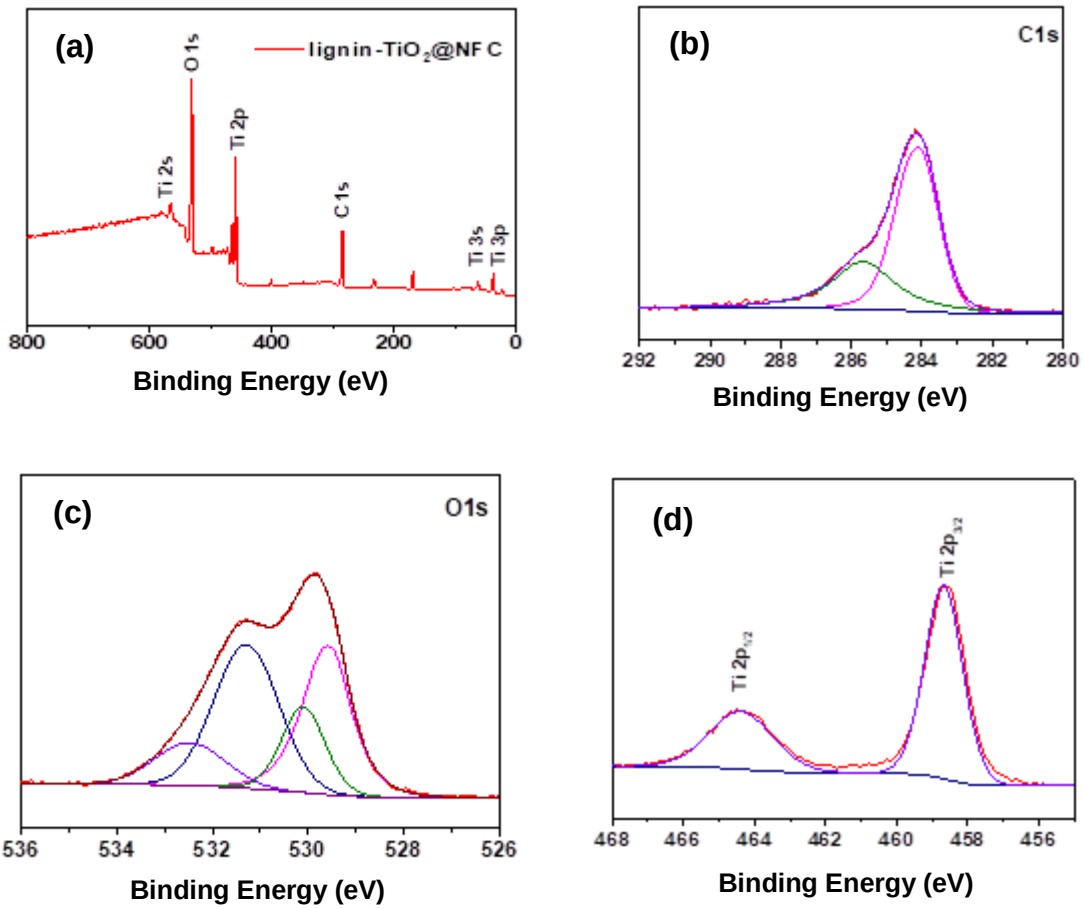

Fig. 7. (a) XPS survey spectra of lignin-TiO_2@NFC. High resolution of XPS spectra for (b) C1s, (c) O1s, and (d) Ti2p

The O1s spectra show a chemical linkage between lignin, NFC, and TiO_2. Peaks at 529.3 and 531.5 eV correspond to Ti-O-Ti bonds and surface hydroxyl groups, respectively, while those at 529.8 and 532.9 eV are classified as C-O-Ti bonds and C-O bonds, respectively (Yu *et al.* 2018). The Ti2p spectrum of the lignin-TiO_2@NFC contains peaks for Ti2p3/2 and Ti2p1/2 located at 458.6 and 464.4 eV, respectively, but they are shifted to lower binding energies than pure TiO_2. This indicates that C-O-Ti bonds in the lignin-

TiO_2@NFC, which lowers the energy of the Ti peak, indicating that some degree of molecular interactions exist between the lignin-TiO_2@NFC (Yang *et al.* 2018). The presence of C-Ti-O bonds demonstrates that lignin was coated on the surface of TiO_2 by esterification-based dehydration condensation. The XPS results also confirmed the preparation mechanism of the novel lignin-TiO_2 induced with NFC, as shown in Fig. 6.

Thermal Analysis

The thermal stabilities of the prepared composite materials were tested by TG. Figure 8 shows that the TiO_2@NFC sample mainly suffered from severe weight loss at approximately 300 °C, which was largely due to the degradation of NFC. Figure 9 shows that the lignin-TiO_2@NFC sample also suffered from severe weight loss at approximately 300 °C, whereas TiO_2 remained stable above 500 °C.

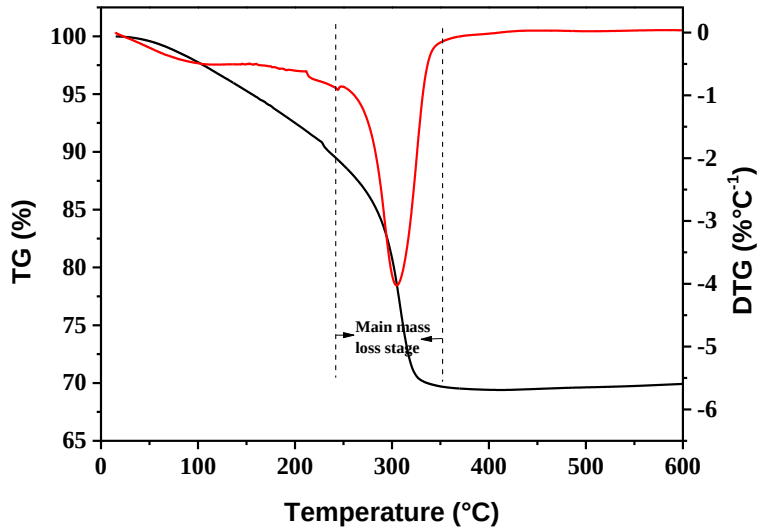

Fig. 8. The TG and DTG curves of the prepared TiO_2@NFC

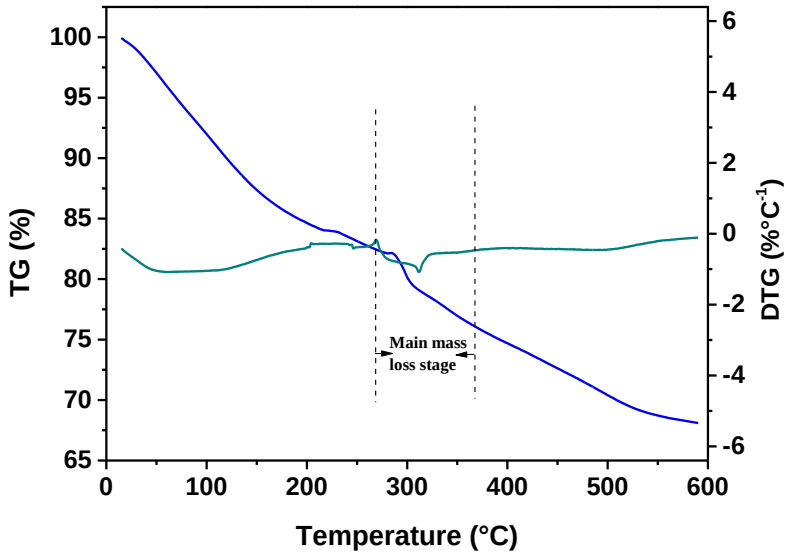

Fig. 9. The TG and DTG curves of the prepared lignin-TiO_2@NFC

The char residue of lignin-TiO_2@NFC at 600 ℃ was 68.1 wt%, which indicated that the lignin-TiO_2@NFC had better thermal stability, and the load of lignin-TiO_2@NFC was approximately 31.9%. The results showed that the thermal stability of lignin-TiO_2@NFC was similar to that reported by Wu *et al*. (2019) but differed from that of TiO_2@NFC and lignin, which showed a relatively stable decline. This indicated that lignin-TiO_2@NFC was not simply a physical combination of TiO_2@NFC and lignin but rather a stable chemical bond.

UV-blocking Performance

TiO_2 is the most commonly used physical sunscreen. Lignin-TiO_2 is both a macromolecular dispersant and a natural sun blocker. Coating lignin on the surface of TiO_2 can improve its dispersity and enhance its UV-blocking property. Therefore, the sunscreen performance of lignin-TiO_2 was investigated and compared with TiO_2 and the unmodified cream physical mixture. The cream matrix was mixed with 5 wt% TiO_2@NFC, 10 wt% lignin-TiO_2@NFC, and 15 wt% lignin-TiO_2@NFC for 8 h until the composite materials were evenly dispersed. The sunscreen performance of lignin-TiO_2 was investigated and compared with TiO_2 and the unmodified cream physical mixture. The cream matrix was mixed with 5 wt% TiO_2@NFC, 5 wt% lignin-TiO_2@NFC, 10 wt% lignin-TiO_2@NFC, and 15 wt% lignin-TiO_2@NFC. The cream matrix mixtures with 5 wt% TiO_2@NFC, 5 wt% lignin-TiO_2@NFC, 10 wt% lignin-TiO_2@NFC, and 15 wt% lignin-TiO_2@NFC were all faint yellow, which was lighter than the color of commonly used BB and therefore acceptable (Fig. 10).

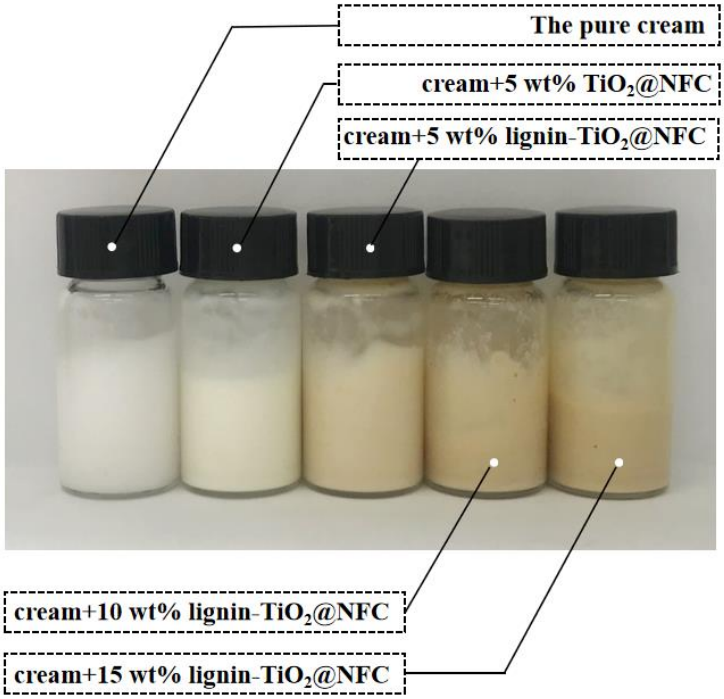

Fig. 10. Image of the unmodified hand cream with 5 wt% TiO_2@NFC and the 5 wt% lignin-TiO_2@NFC, 10 wt% lignin-TiO_2@NFC, and 15 wt% lignin-TiO_2@NFC physical mixtures

Figure 11 shows the typical UV transmittance of the unmodified hand cream and the cream blended with 5 wt% TiO_2@NFC and 5 wt% lignin-TiO_2@NFC in the UVA and UVB areas. The unmodified hand cream exhibited poor UV-blocking performance and higher transmittance. With the same 5% concentration, the transmittance of lignin-TiO_2@NFC was lower than that of TiO_2@NFC in the UVA areas, whereas the transmittance of lignin-TiO_2@NFC was close to TiO_2@NFC in the UVB areas. Due to the presence of chromophore groups in the lignin which reduces the light transmittance of composite materials. The lignin-TiO_2@NFC significantly reduces the UVA (320 nm to 400 nm) and UVB (280 nm to 320 nm) transmittance because of the uniform distribution and synergistic effect between the TiO_2 and lignin components (Rukmanikrishnan *et al.* 2020). Therefore, the UV shielding effect of lignin-TiO2@NFC was superior.

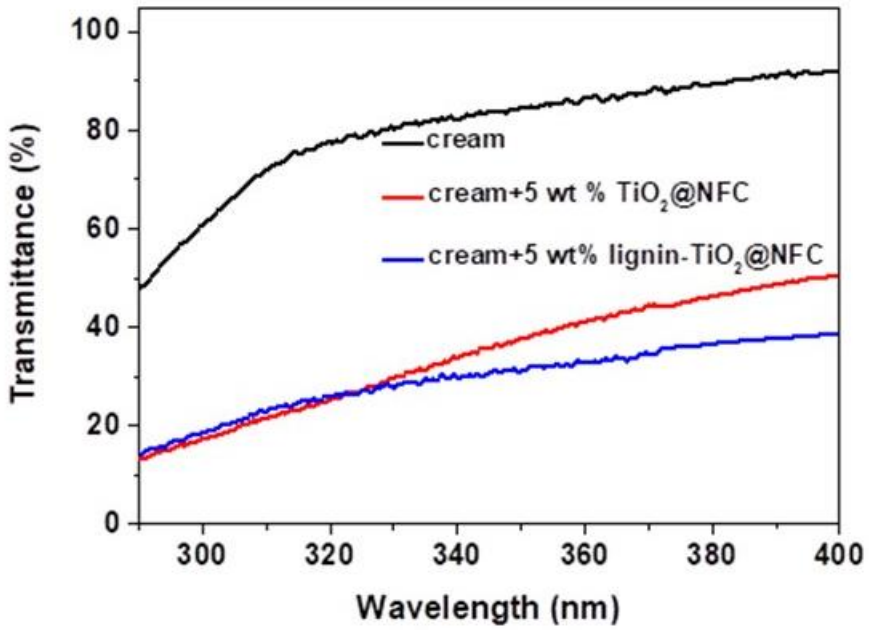

Fig. 11. Typical UV transmittance of the unmodified hand cream and the cream blended with 5 wt% TiO_2@NFC and 5 wt% lignin-TiO_2@NFC and the physical mixture in the UVA and UVB areas

Then, the typical UV transmittance of the unmodified hand cream and the cream blended with 5 wt% lignin-TiO_2@NFC, 10 wt% lignin-TiO_2@NFC, and 15 wt% lignin-TiO_2@NFC in the UVA and UVB areas were studied. Figure 12 shows that, as input amount increased, the UV shielding effect became more obvious. Compared to 5 wt% lignin-TiO_2@NFC, the input amount of 10 wt% lignin-TiO_2@NFC was greatly improved, whereas the effects of 10 wt% lignin-TiO_2@NFC and 15 wt% lignin-TiO_2@NFC were similar. However, higher dosages of composite materials would demulsify the sun cream, and the 15 wt% input amounts of the nanocomposites dispersed well in the unmodified hand cream. In addition, 10 wt% lignin-TiO_2@NFC was the best dosage, and it could absorb approximately 90% of UV light in the full UV band (200 nm to 400 nm), which indicated the lignin-TiO_2@NFC had a good UV-shielding property.

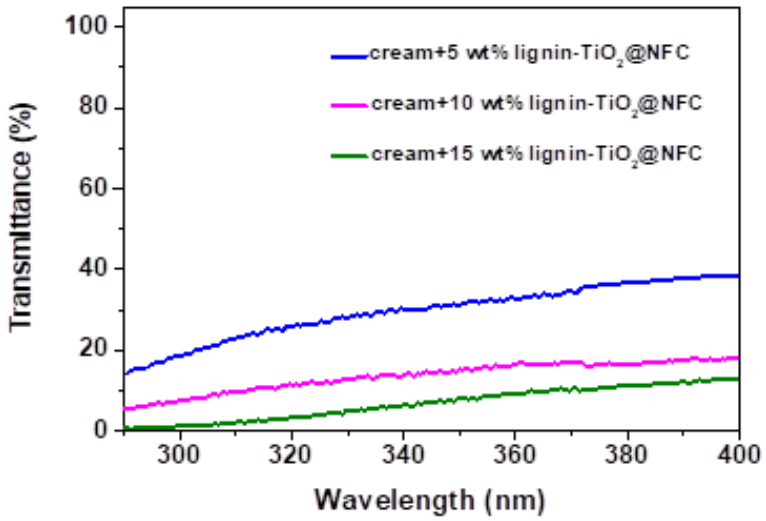

Fig. 12. Typical UV transmittance of hand cream blended with 5 wt% lignin-TiO_2@NFC, 10 wt% lignin-TiO_2@NFC, and 15 wt% lignin-TiO_2@NFC and the physical mixture in the UVA and UVB areas

CONCLUSIONS

1. In this work, a novel lignin-TiO_2 UV-shielding composite was synthesized successfully *via* a hydrothermal method induced with NFC, and the TiO_2 was synthesized *via* the same method without the addition of lignin.
2. Comparison of the characterization results of TiO_2 and lignin-TiO_2 showed that the lignin-TiO_2@NFC had anatase nanoparticles with good thermal stability.
3. The UV-vis transmission spectra results revealed that the unmodified hand cream containing 10 wt% lignin-TiO_2@NFC could absorb approximately 90% of UV light in the full UV band (200 nm to 400 nm), which indicated that the lignin-TiO_2 induced by NFC had a good UV-shielding property.

ACKNOWLEDGMENTS

This work was supported by the Zhejiang Province Natural Science Foundation of China (Grant No. LY20C160006), the Key Special Subject of Science and Technology Program of Zhejiang Province (Grant No. 2020C02043), the International Cooperative Research Project (Grant No. 2016YEE0125800), the National Natural Science Foundation of China (Grant No. 31500492), and the Open Fund of the Key Laboratory of Pulp and Paper Science and Technology of Ministry of Education of China at Qilu University of Technology (Grant No. KF201824).

REFERENCES CITED

An, G., Ma, W., Sun, Z., Liu, Z., Han, B., Miao, S., Miao, Z., and Ding, K. (2007). "Preparation of titania/carbon nanotube composites using supercritical ethanol and

their photocatalytic activity for phenol degradation under visible light irradiation," *Carbon* 45(9), 1795-1801. DOI: 10.1016/j.carbon.2007.04.034

Chen, X., Kuo, D.-H., and Lu, D. (2016a). "N-doped mesoporous TiO_2 nanoparticles synthesized by using biological renewable nanocrystalline cellulose as template for the degradation of pollutants under visible and sun light," *Chemical Engineering Journal* 295, 192-200. DOI: 10.1016/j.cej.2016.03.047

Chen, X., Kuo, D.-H., Lu, D., Hou, Y., and Kuo, Y.-R. (2016b). "Synthesis and photocatalytic activity of mesoporous TiO_2 nanoparticle using biological renewable resource of un-modified lignin as a template," *Microporous and Mesoporous Materials* 223, 145-151. DOI: 10.1016/j.micromeso.2015.11.005

Chen, K., Lei, L., Qian, Y., Xie, A., and Qiu, X. (2019). "Biomass lignin stabilized anti-UV high internal phase emulsions: Preparation, rheology, and application as carrier materials," *ACS Sustainable Chemistry & Engineering* 7(1), 810-818. DOI: 10.1021/acssuschemeng.8b04422

Chu, S., Miao, Y., Qian, Y., Ke, F., Chen, P., Jiang, C., and Chen, X. (2019). "Synthesis of uniform layer of TiO_2 nanoparticles coated on natural cellulose micrometer-sized fibers through a facile one-step solvothermal method," *Cellulose* 26(8), 4757-4765. DOI: 10.1007/s10570-019-02425-w

Dong, L., Liu, X., Xiong, Z., Sheng, D., Zhou, Y., Lin, C., and Yang, Y. (2018). "Design of UV-absorbing PVDF membrane *via* surface-initiated AGET ATRP," *Applied Surface Science* 435, 680-686. DOI: 10.1016/j.apsusc.2017.11.135

Dinh, C.-T., Nguyen, T.-D., Kleitz, F., and Do, T.-O. (2009). "Shape-controlled synthesis of highly crystalline titania nanocrystals," *ACS Nano* 3(11), 3737-3743. DOI: 10.1021/nn900940p

Giese, M., Blusch, L. K., Khan, M. K., and MacLachlan, M. J. (2015). "ChemInform abstract: Functional materials from cellulose-derived liquid-crystal templates," *Angew. Chem. Int. Ed.* 54, 2888-2910. DOI: 10.1002/anie.201407141

Hambardzumyan, A., Foulon, L., Chabbert, B., and Aguié-Béghin, V. (2012). "Natural organic UV-absorbent coatings based on cellulose and lignin: Designed effects on spectroscopic properties," *Biomacromolecules* 13(12), 4081-4088. DOI: 10.1021/bm301373b

Hu, Y., Ge, J., Sun, Y., Zhang, T., and Yin, Y. (2007). "A self-templated approach to TiO_2 microcapsules," *Nano Letters* 7(6), 1832-1836. DOI: 10.1021/nl0708157

Ibrahim, M. N. M., Iqbal, A., Shen, C. C., Bhawani, S. A., and Adam, F. (2019). "Synthesis of lignin-based composites of TiO_2 for potential application as radical scavengers in sunscreen formulation," *BMC Chemistry* 13(1), Article number 17. DOI: 10.1186/s13065-019-0537-3

Jaroenworaluck, A., Sunsaneeyametha, W., Kosachan, N., and Stevens, R. (2006). "Characteristics of silica-coated TiO_2 and its UV absorption for sunscreen cosmetic applications," *Surface and Interface Analysis* 38(4), 473-477. DOI: 10.1002/sia.2313

Kai, D., Tan, M. J., Chee, P. L., Chua, Y. K., Yap, Y. L., and Loh, X. J. (2016). "Towards lignin-based functional materials in a sustainable world," *Green Chemistry* 18(5), 1175-1200. DOI: 10.1039/C5GC02616D

Li, Y., Chen, C., Li, J., and Sun, X. S. (2011). "Synthesis and characterization of bionanocomposites of poly(lactic acid) and TiO_2 nanowires by *in situ* polymerization," *Polymer* 52(11), 2367-2375. DOI: 10.1016/j.polymer.2011.03.050

Li, Z., Zhang, J., Qin, L., and Ge, Y. (2018). "Enhancing antioxidant performance of lignin by enzymatic treatment with laccase," *ACS Sustainable Chemistry & Engineering* 6(2), 2591-2595. DOI: 10.1021/acssuschemeng.7b04070

Li, Y., Yang, D., Lu, S., Qiu, X., Qian, Y., and Li, P. (2019). "Encapsulating TiO_2 in lignin-based colloidal spheres for high sunscreen performance and weak photocatalytic activity," *ACS Sustainable Chemistry & Engineering* 7(6), 6234-6242. DOI: 10.1021/acssuschemeng.8b06607

Marques, P. A. A. P., Trindade, T., and Neto, C. P. (2006). "Titanium dioxide/cellulose nanocomposites prepared by a controlled hydrolysis method," *Composites Science and Technology* 66(7-8), 1038-1044. DOI: 10.1016/j.compscitech.2005.07.029

Miao, S., Miao, Z., Liu, Z., Han, B., Zhang, H., and Zhang, J. (2006). "Synthesis of mesoporous TiO_2 films in ionic liquid dissolving cellulose," *Microporous and Mesoporous Materials* 95(1-3), 26-30. DOI: 10.1016/j.micromeso.2006.04.013

Morlando, A., Sencadas, V., Cardillo, D., and Konstantinov, K. (2018). "Suppression of the photocatalytic activity of TiO_2 nanoparticles encapsulated by chitosan through a spray-drying method with potential for use in sunblocking applications," *Powder Technology* 329, 252-259. DOI: 10.1016/j.powtec.2018.01.057

Morsella, M., D'Alessandro, N., and Lanterna, A. E. (2016). "Improving the sunscreen properties of TiO_2 through an understanding of its catalytic properties," *ACS Omega* 1(3), 464-469. DOI: 10.1021/acsomega.6b00177

Nair, V., Dhar, P., and Vinu, R. (2016). "Production of phenolics *via* photocatalysis of ball milled lignin–TiO_2 mixtures in aqueous suspension," *RSC Advances* 6(22), 18204-18216. DOI: 10.1039/C5RA25954A

Pan, X., Kadla, J. F., Ehara, K., Gilkes, N., and Saddler, J. N. (2006). "Organosolv ethanol lignin from hybrid poplar as a radical scavenger: Relationship between lignin structure, extraction conditions, and antioxidant activity," *Journal of Agricultural and Food Chemistry* 54(16), 5806-5813. DOI: 10.1021/jf0605392

Qian, Y., Qiu, X., and Zhu, S. (2016). "Sunscreen performance of lignin from different technical resources and their general synergistic effect with synthetic sunscreens," *ACS Sustainable Chemistry & Engineering* 4(7), 4029-4035. DOI: 10.1021/acssuschemeng.6b00934

Rockafellow, E. M., Stewart, L. K., and Jenks, W. S. (2009). "Is sulfur-doped TiO_2 an effective visible light photocatalyst for remediation?," *Applied Catalysis B: Environmental* 91(1-2), 554-562. DOI: 10.1016/j.apcatb.2009.06.027

Rukmanikrishnan, B., Rajasekharan, S. K., Lee, J., Ramalingam, S., and Lee, J. (2020). "K-Carrageenan/lignin composite films: Biofilm inhibition, antioxidant activity, cytocompatibility, UV and water barrier properties," *Material Today*, communication 101346. DOI: 10.1016/j.mtcomm.2020.101346

Sambandan, D. R., and Ratner, D. (2011). "Sunscreens: An overview and update," *Journal of The American Academy of Dermatology* 64(4), 748-758. DOI: 10.1016/j.jaad.2010.01.005

Sander, C. S., Chang, H., Salzmann, S., Müller, C. S. L., Ekanayake-Mudiyanselage, S., Elsner, P., and Thiele, J. J. (2002). "Photoaging is associated with protein oxidation in human skin *in vivo*," *Journal of Investigative Dermatology* 118(4), 618-625. DOI: 10.1046/j.1523-1747.2002.01708.x

Shen, B., Scaiano, J. C., and English, A. M. (2006). "Zeolite encapsulation decreases TiO_2-photosensitized ROS generation in cultured human skin fibroblasts," *Photochemistry and Photobiology* 82(1), 5-12. DOI: 10.1562/2005-05-29-RA-551

Slaper, H., Velders, G. J. M., Daniel, J. S., De Gruijl, F. R., and Van der Leun, J. C. (1996). "Estimates of ozone depletion and skin cancer incidence to examine the Vienna Convention achievements," *Nature* 384(6606), 256-258. DOI: 10.1038/384256a0

Sun, S.-L., Wen, J.-L., Ma, M.-G., Sun, R.-C., and Jones, G. L. (2014). "Structural features and antioxidant activities of degraded lignins from steam exploded bamboo stem," *Industrial Crops Prod.* 56(3), 128-136. DOI: 10.1016/j.indcrop.2014.02.031

Wei, L., Ying, Z., and Shouxin, L. (2012). "Mesoporous TiO_2 spheres prepared by an acid catalyzed hydrolysis method using nanocrystalline cellulose as template," *Chinese Journal of Catalysis* 33(2), 342-347. DOI: 10.3724/SP.J.1088.2012.10864

Wu, W., Liu, T., Deng, X., Sun, Q., Cao, X., Feng, Y., Wang, B., Roy, V. A. L., and Li, R. K. Y. (2019). "Ecofriendly UV-protective films based on poly(propylene carbonate) biocomposites filled with TiO_2 decorated lignin," *International Journal of Biological Macromolecules* 126, 1030-1036. DOI: 10.1016/j.ijbiomac.2018.12.273

Xiao, J., Chen, W., Wang, F., and Du, J. (2013). "Polymer/TiO2 hybrid nanoparticles with highly effective UV-screening but eliminated photocatalytic activity," *Macromolecules* 46(2), 375-383. DOI: 10.1021/ma3022019

Yang, D., Wang, S., Zhong, R., Liu, W., and Qiu, X. (2018). "Preparation of lignin/tio2 nanocomposites and their application in aqueous polyurethane coatings," *Frontiers of Chemical Science and Engineering* 13(1):59-69. DOI: 10.1007/s11705-018-1712-0

Yu, J., Li, L., Qian, Y., Lou, H., and Qiu, X. (2018). "Facile and green preparation of high uv-blocking lignin/titanium dioxide nanocomposites for developing natural sunscreens," *Industrial & Engineering Chemistry Research* 57(46). DOI: 10.1021/acs.iecr.8b04101

Zaccariello, G., Back, M., Zanello, M., Canton, P., Cattaruzza, E., Riello, P., Alimonti, A., and Benedetti, A. (2017). "Formation and controlled growth of bismuth titanate phases into mesoporous silica nanoparticles: An efficient self-sealing nanosystem for UV filtering in cosmetic formulation," *ACS Applied Materials & Interfaces* 9(2), 1913-1921. DOI: 10.1021/acsami.6b13252

Zhou, W., and Fu, H. (2013). "Mesoporous TiO_2: Preparation, doping, and as a composite for photocatalysis," *ChemCatChem* 5(4), 885-894. DOI: 10.1002/cctc.201200519

Zhou, Y., Ding, E.-Y., and Li, W.-D. (2007). "Synthesis of TiO_2 nanocubes induced by cellulose nanocrystal (CNC) at low temperature," *Materials Letters* 61(28), 5050-5052. DOI: 10.1016/j.matlet.2007.04.001

Zhang, Y., Liu, Y., Ge, C., Yin, H., Ren, M., Wang, A., Jiang, T., and Yu, L. (2009). "Evolution mechanism of alumina nanofilms on rutile TiO_2 starting from sodium metaaluminate and the pigmentary properties," *Powder Technology* 192(2), 171-177. DOI: 10.1016/j.powtec.2008.12.009

Zhang, C., Uchikoshi, T., Ichinose, I., and Liu, L. (2019). "Surface modification on cellulose nanofibers by TiO_2 coating for achieving high capture efficiency of nanoparticles," *Coatings* 9(2), Article number 139. DOI: 10.3390/coatings9020139

Article submitted: June 1, 2020; Peer review completed: July 25, 2020; Revised version received and accepted: Aug. 1, 2020; Published: August 7, 2020.
DOI: 10.15376/biores.15.4.7374-7389